

Flight Testing of Mission Adaptive Compliant Wing

Joel Hetrick* and Russell Osborn† and Sridhar Kota‡
FlexSys Inc., Ann Arbor, MI, 48105

and

Peter Flick§ and Donald Paul**
Air Force Research Laboratory, Dayton, OH, 45433

This paper describes flight testing of a “Mission Adaptive Compliant Wing” (MACW) adaptive structure trailing edge flap used in conjunction with a natural laminar flow airfoil. The MACW technology provides light-weight, low power, variable geometry re-shaping of the upper and lower flap surface with no seams or discontinuities. In this particular study, the airfoil-flap system is optimized to maximize the laminar boundary layer extent over a wide lift coefficient range for endurance aircraft applications. The expanded “laminar bucket” capability allows the endurance aircraft to significantly extend their range by continuously optimizing the wing L/D throughout the mission. The wing was tested at full-scale dynamic pressure, full scale Mach, and reduced-scale Reynolds Numbers on the Scaled Composites White Knight aircraft. Testing revealed low drag levels and laminar flow to at approximately 60% chord for much of the lift range. Airfoil predictions are compared to MSES computational results.

Nomenclature

A	=	aspect ratio
C_P	=	pressure coefficient
C_L	=	lift coefficient
C_M	=	quarter chord moment coefficient
g_2	=	total pressure in airfoil wake region
g_∞	=	ambient total pressure
M_∞	=	Mach number
p_2	=	static pressure in airfoil wake region
p_∞	=	ambient static pressure
q_∞	=	ambient dynamic pressure
α	=	angle of attack
α'	=	reduced angle of attack due to wing aspect ratio
γ	=	specific heat ratio of air = 1.4

I. Introduction

Working with funding supplied by the AFRL, Air Vehicles Directorate, FlexSys Inc. has developed a unique, variable-geometry, trailing edge flap that can re-contour the airfoil upper and lower surface. Since the weight of long endurance aircraft can vary significantly over the course of a mission, the ability to minimize drag across a wide operating lift coefficient range provides a significant performance advantage for any aircraft that incorporates the compliant flap technology. FlexSys has applied the compliant flap system to an aggressive Natural Laminar Flow (NLF) airfoil developed for SensorCraft applications. This airfoil can theoretically achieve up to 65% chord laminar flow on the upper surface and up to 90% chord laminar flow on the lower surface. Because NLF airfoils with long laminar runs have steep pressure gradients in the pressure recovery region, the gentle curvature change

* Vice President, 2006 Hogback Rd., Suite 7, Ann Arbor, MI 48105.

† Aero Specialist, PO Box 1427, Russells Point, OH 433348, AIAA Member.

‡ President, 2006 Hogback Rd., Suite 7, Ann Arbor, MI 48105.

§ Program Manager, AFRL/VAAA, 2130 8th St. WPAFB, OH 45533-7542.

** Chief Scientist, AFRL/VAAA, 2130 8th St. WPAFB, OH 45533-7542.

provided by a compliant flap can reduce or eliminate flow separation over the flap surface as opposed to a rotational flap which can separate flow at the flap knee. Analyses and flight testing indicate that these long laminar runs can be maintained while the compliant trailing edge flap is deflected.

A. Mission Adaptive Compliant Wing Technology

In contrast to conventional elastic mechanisms, or flexures, that employ flexible hinges, the Mission Adaptive Compliant Wing (MACW) wing uses sophisticated algorithms to design the topology and shape of an internal structure that deforms as a whole rather than concentrating the flexion in localized regions that can create high-stress concentrations. This new design paradigm offers additional benefits since the whole adaptive structure is viewed as a compliant mechanism [REF] that can move into complex predetermined positions with only minimal force and be locked in place at any desired configuration. While the structures are described as “flexible”, they are optimized to resist deflection under external aerodynamic loading and are actually quite stiff and strong. The elimination of discontinuities in the flap surface can provide lower drag and higher control authority than comparable hinged flaps. Further, the elimination of joints and seams can provide a signature reduction and also make the surface more impervious to icing and fouling due to dirt and debris.

While the current research focuses on a trailing edge adaptive structure, the development of morphing surfaces for both the leading and trailing edge; and for both fixed wing and rotorcraft airfoils is ongoing. Research is targeted to minimizing the force required to morph surfaces during the full flight profile while maintaining maximum stiffness to withstand external loading. Since the project has progressed, design and optimization algorithms can account for: actuator motion, morphing shape error, overall system weight, buckling forces and package constraints in addition to overall system complexity and material fatigue. Currently, several iterations are necessary to resolve conflicting design requirements between the aeroelastic behavior and the compliant structure design. Several models have been built and tested to look at aerodynamic performance as well as structural performance.

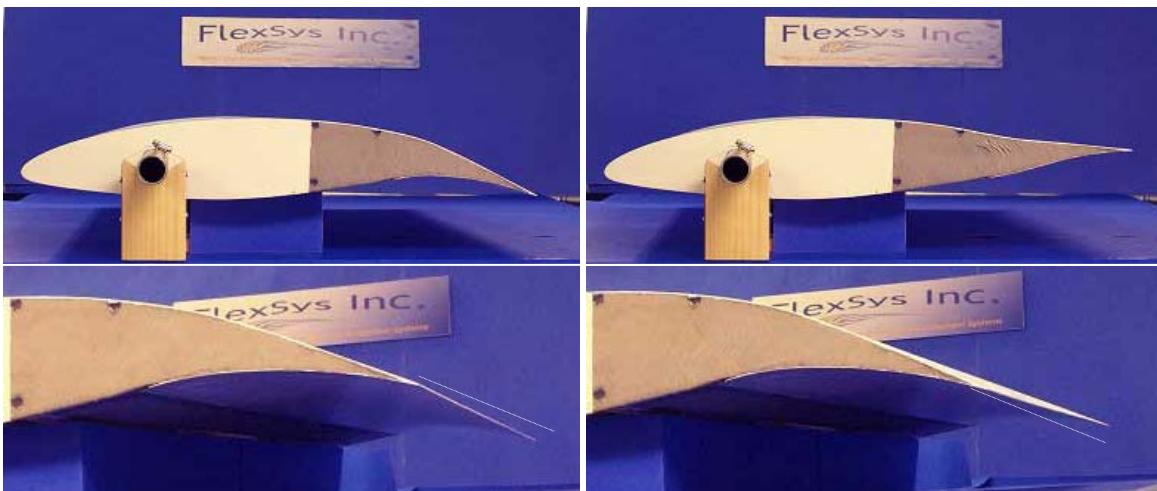


Figure 1. Flexsys Inc.’s Mission Adaptive Compliant Wing trailing edge designed for a high altitude long endurance aircraft undergoing +/- 10-degree flap deflection with a 3-degree twist. The airfoil and the conformal flap combination were designed to support an aggressive, 65% laminar boundary layer (chord-wise) on the upper surface.

In order to produce motion, a MACW flap must elastically strain the flap structure. The required energy to re-shape the structure is minimized during optimization. Even with the additional force required to elastically deform the structure, these flaps work against the aerodynamic loading differently than a hinged flap. Comparing the peak power draw during a high rate movement, MACW flaps can actually require less force and less power than a comparably sized conventional flap. One study comparing MACW to conventional trailing edge flaps during a max G pull-up maneuver showed that the MACW variable camber flaps actually required 30% less actuation force and 17% lower peak actuator power.

The aerodynamic benefits of the smooth variable camber structures are significant. Comparing equal sized trailing edge control surfaces, MACW flaps can provide up to a 40% increase in control authority per degree deflection over hinged control surface. These gains can be realized with up to 25% lower drag. The boost in aerodynamic performance occurs not only at the aft portion where the trailing edge is located, but over the entire

airfoil chord. Forward of the trailing edge, the increased performance is a result of increased circulation and elevated leading edge suction (stagnation point control) created by the variable geometry technology. Figure 2 (a) illustrates aerodynamic analysis of a MACW trailing edge flap performed in XFOIL, note that laminar flow is maintained for a longer chord percentage for the MACW flap as compared to the plain rotating flap. Figure 2 (b) illustrates a direct comparison of the conventional flap L/D performance compared to the MACW flap L/D performance. In some cases the MACW flap achieves nearly a 75% increase in L/D.

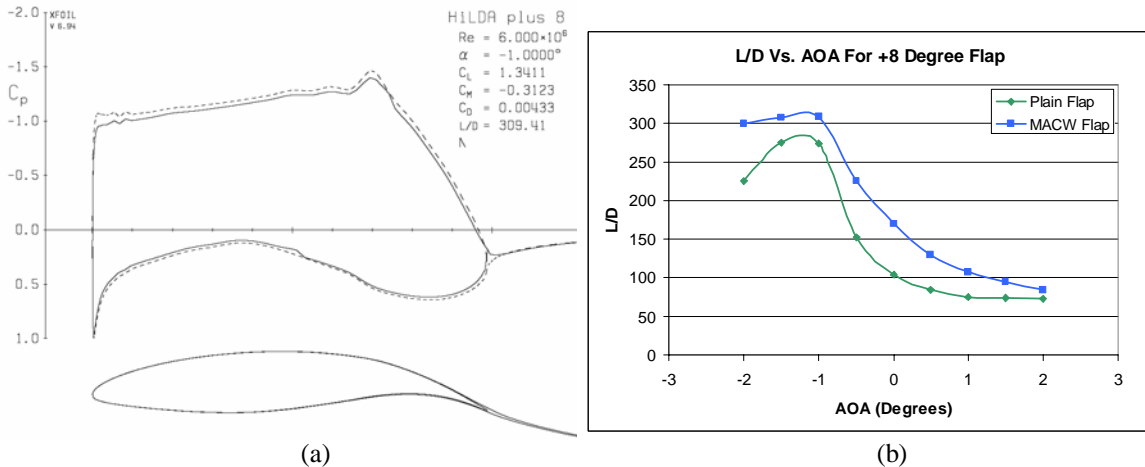


Figure 2. (a) XFOIL analysis of a plain flap with a +8 degree flap deflection. (b) XFOIL analysis showing L/D comparison of a plain flap and a MACW flap at +8 degree flap deflection.

The composition of the MACW structure is currently aircraft grade aluminum. These structures are estimated to weigh roughly 30% more than an all-up composite conventional hinged flap. Progression to a full composite MACW flap is underway and is estimated to provide significant reductions in weight (20% to 30% weight reduction) as well as gains in strength and allowable deflection range.

Finally, MACW technology allows the flap to be positioned with a linearly varying flap deflection along the wing span. Extensive simulation under aerodynamic loading, wing flex, and flap twist (Figure 3) illustrated that these structures can safely withstand these multitude of loads while keeping material strains well within their cyclic limits. This differential deflection capability allows a vehicle equipped with MACW flaps to create subtle adjustments to the spanwise lift distribution. This has the benefit of allowing the flap to reshape the wing lift distribution closer to an elliptical distribution, minimizing induced drag, and/or by reducing the lift levels on outboard sections of the wing in order to minimize the wing root bending moment – thus potentially saving weight.

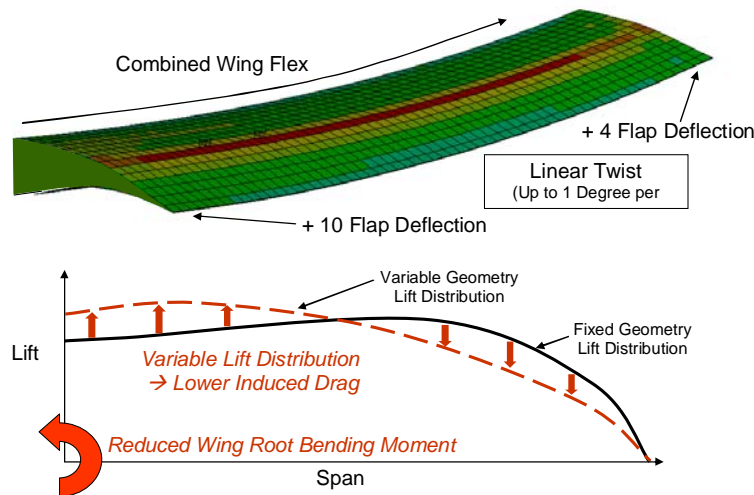


Figure 3. Capability of the MACW control surfaces to produce differential deflection along the span of a wing thereby providing spanwise load tailoring for wing root bending moment control and lift distribution control.

B. High-Altitude Long Endurance “SensorCraft” Application

The U.S. Air Force Research Laboratory (AFRL) has identified certain feasible vehicle concepts and aerodynamic technology development requirements for a high-altitude long-endurance intelligence-surveillance-reconnaissance (ISR) concept vehicle known as SensorCraft [REF A]. SensorCraft is conceived as an unmanned air vehicle system performing command, control, detection, identification, tracking, relay, and targeting functions for long durations at extended ranges. It is the air-breather component of a fully integrated intelligence, surveillance, and reconnaissance (ISR) enterprise that incorporates air, space, and ground components.

MACW adaptive structures technology allows the airfoil profile to be tailored to the transitory flight condition (Mach number, wing loading, etc.) over the entire mission. When a natural laminar flow (NLF) airfoil is forced to operate at a higher wing loading (higher lift coefficient) than it is designed for, the leading edge stagnation point moves further aft on the underside of the airfoil and a large suction peak is created as the flow accelerates around the leading edge. This ultimately results in a significantly adverse pressure gradient over the forward part of the upper surface. This forces the boundary layer to transition to turbulent – after which it grows significantly and often creates trailing edge separation as well. This separation is illustrated in Figure 4 (a) for an airfoil optimized for L/D at $CL=1.0$ is forced to operate at $CL=1.2$. A typical SensorCraft platform is expected to burn over half of its weight in fuel, while the cruise-climb method of staying near the design lift coefficient will be severely limited by altitude limitations on the engine(s), and could be constrained by sensor operations. Figure 4 (b) illustrates the potential benefits of using variable geometry compliant structures to produce small, smooth deflections of the trailing edge of a Natural Laminar Flow (NLF) airfoil designed for a representative SensorCraft. Small deflections of the adaptive trailing edge are used to expand the laminar low-drag bucket by controlling the location of the stagnation point and hence the pressure gradient at off-design conditions. This can allow the entire mission to be performed at a reasonably high L/D.

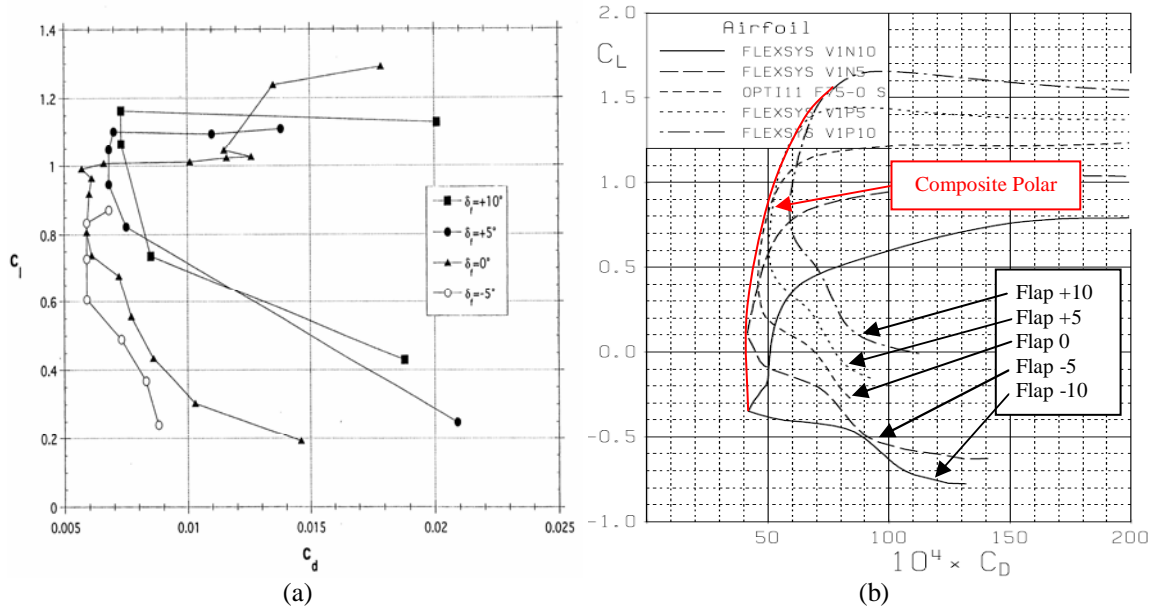


Figure 4. (a) CL Vs. CD data for a modern long endurance airfoil with a conventional trailing edge flap [REF]. (b) CFD plot from MSES showing the composite polar for the MACW flap.

II. Flight Test Model Description

The purpose of this test program is to quantify the aerodynamic and structural performance of a representative Mission Adaptive Compliant Wing (MACW) prototype system designed for high altitude, long endurance aircraft applications subject to relevant flight environments. The MACW prototype system is flight-tested using the Scaled Composite's White Knight aircraft that is capable of flying at altitude and Mach conditions compatible with long endurance aircraft operations. The prototype model is designed for an aggressive, 65% chord, laminar boundary layer run on the upper surface that must be maintained over a range of operating lift coefficients using subtle MACW flap deflections. Relevant test conditions are best re-created in the low ambient turbulence, high altitude, flight test environment.

C. Model Description

The MACW model is shown in Figure 5. The wing has a 50 inches span and 30 inch chord (aspect ratio of 1.67). Elliptical endplates (45" x 24") help bound the flow and reduce three-dimensional effects. The wing is mounted in a cantilever arrangement with all loads channeled through one primary mount (at the bottom of Figure 5). The wing is capable of generating significant force; however, testing is limited to a maximum CL of 1.2 (roughly 950 lb of lift at flight test condition of 83 psf).

From 70% to 100% of the model chord is a structurally optimized variable camber flap driven by two electrical servo motors. The flap is capable of +/-10 degree change in camber (flap deflection) at rates up to 30 degrees per second (loaded). The upper surface of the flap consists of a smooth, continuous surface of an aluminum and polymer composition. The lower surface uses the same composition with an additional composite reinforced elastomer panel extending from roughly 65% to 75% of the model chord.

The leading edge of the flight test model is directly machined from 7075-T6 aluminum and holds tolerances as tight as +/- 0.0005" within the first 5% of the model chord. The surface of the model leading edge was ground to better than a 6 mil surface finish. The model incorporates an angle of attack servo system and a swing arm wake rake servo system. The aluminum leading edge is directly bolted to a heavy duty turntable bearing that securely fastens the wing to a fixed steel mounting plate. A linear actuator and pivot arrangement is located 15" radially from the turntable bearing center and controls the model angle of attack. A separate servo motor rotates the wake arm to sweep through the airfoil wake region (sweeps across the airfoil height).

With the exception of the compliant trailing edge flap and the wake link, all structural components maintain safety factors of 8 or greater. The compliant trailing edge flap, due to its need to elastically strain, maintains a static loading safety factor of 2; however, the safety factor with respect to fatigue cyclic loading of this component is considerable (greater than 50).

The MACW model was hung from the vertical stub pylon located on the underbelly of the Scaled Composites White Knight. Figure 6 shows the White Knight with the MACW model. During take off and landing, the ground clearance from the air data boom of the MACW model to the ground is 20 inches with the tires flat and the landing gear struts fully compressed.



Figure 5: MACW model was tested at the Subsonic Aerodynamic Research Lab at the Wright Patterson Air Force Base (June 2006). Testing at the wind tunnel served to test the model and all aerodynamic instrumentation prior to flight testing.

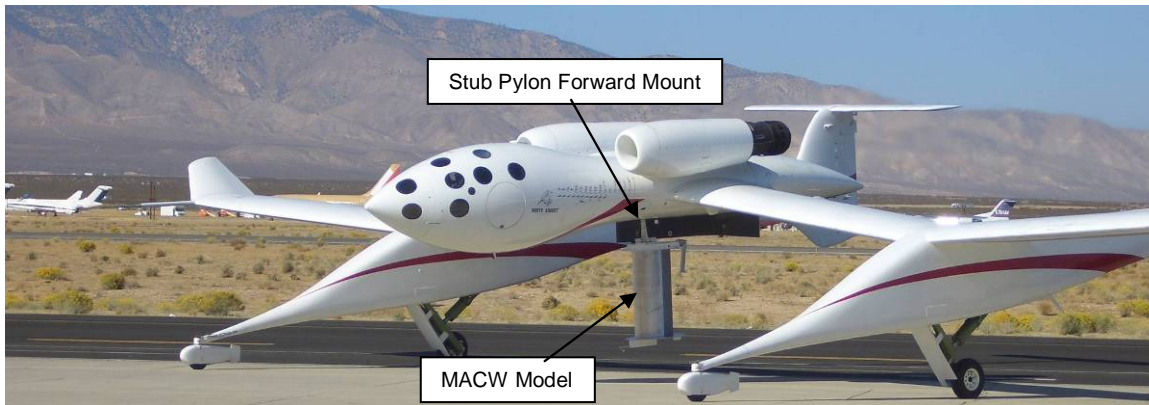


Figure 6. MACW model mounting to Scaled Composites White Knight Aircraft.

D. Instrumentation

The following items represent a brief description of all of the major systems that control, sense, acquire, and store information for the MACW model. Figure 7 shows a schematic of the model data acquisition and control system.

1. *Data acquisition system and model control interface.* A laptop computer serves as the central nervous system to monitor pressures, wake data, hot film data, as well as control angle of attack, the wake rake, and the compliant trailing edge flap servo system. This computer is programmed using Labview and automates many of the data acquisition processes. Two National Instruments 16-bit, 200 kS/sec USB DAQ boards serve as principle data measurement modules. An RS485 card and cables connects all servo motors to the laptop.
2. *Pressure scanners.* One 64 channel and one 32 channel Scanivalve pressure scanning modules are located in the outboard section of the model. A total of 76 0.040" diameter pressure taps – staggered at 15 degrees to prevent upstream laminar flow contamination – are used to record pressure over the surface of the airfoil. Other pressure sensor ports are used to instrument the wake rake and the air data boom. Reference pressure is fed to the pressure scanners from the total pressure port on the air data boom. In addition, information is logged from the White Knight flight computer.
3. *Model angle of attack servo system (model geometric).* A heavy duty turntable bearing is located at 23% chord and rigidly connects the airfoil to the mount plate. This bearing allows AOA rotation while sustaining shear and moment loads due to wing lift. A servo motor is mounted to the fixed mount plate. Using a 50:1 gearhead reduction combined with a ball screw drive system and pivoting mounts, the AOA unit is capable of rotating the model from +2 degrees to +12 degrees angle of attack. Hard stops are built into the unit to prevent further rotation.
4. *Swing arm wake probe.* A wake probe with pitot-static probes is used to measure wake total pressure profiles at all pertinent test conditions. This probe is mounted to the inboard elliptical end plate. The swing arm probe can traverse +/- 45 degrees to measure the airfoil wake deficit.
5. *Hot film sensors.* Fifteen total Dantec Dynamics hot film sensors are arranged to measure the boundary layer transition position. These sensors are mounted on the airfoil upper surface at 24%, 34%, 43%, 48%, 53%, 58%, 63%, 66% and 68% chord position. In addition, hot films are mounted on the lower surface at 24%, 34%, 43%, 48%, 53%, and 58% chord position. Hot film sensors are read using a Dantec Dynamics 8 channel thermal anemometer which is capable of reading frequencies up to 10k Hz.
6. *Air data boom.* A Space Age Control air data boom is mounted off the outboard elliptical end plate. This unit measures static pressure, total pressure, angle-of-attack and angle-of-sideslip information.
7. *Video cameras.* Three remote head video cameras are mounted to the inboard elliptical end plate to view the leading edge, the upper surface of the TE flap and the lower surface of the TE flap. A four-

channel digital video recorder with an LCD monitor are used to view camera output and record testing video.

8. *Accelerometer.* An accelerometer is located at the outboard section at 65% chord to monitor model vibrations during flight testing.
9. *Model power supply system.* A series of DC to DC converters step up or step down DC power from the aircraft 28 VDC bus supply. This power supply system is designed to provide minimal noise for signal sensitive instrumentation while providing enough power for servo systems.

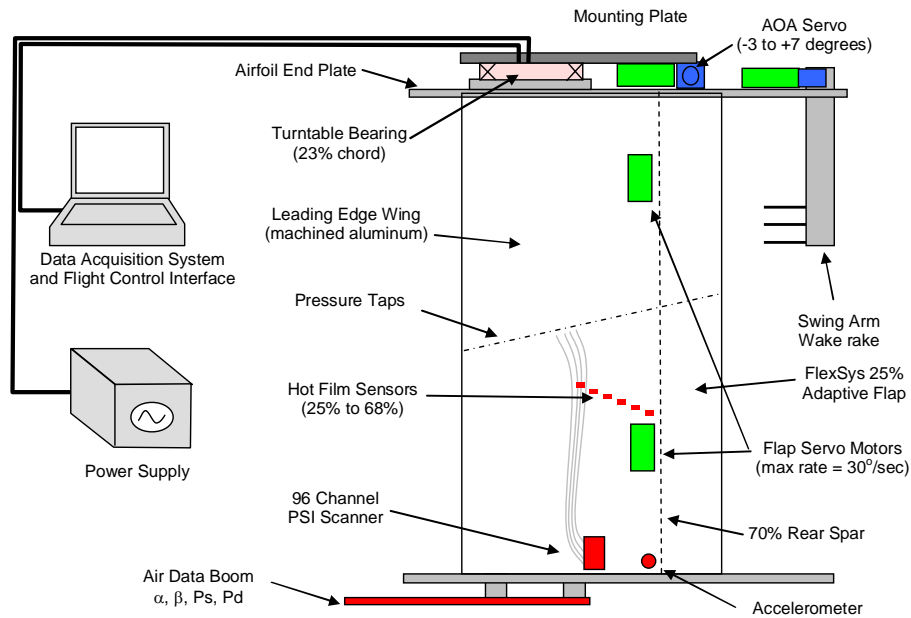


Figure 7. Data Acquisition and Model Control System.

III. Flight Testing Approach

Flight testing was conducted at Scaled Composites facility at the Mojave civilian airport at Mojave, CA. The model was mounted to the underbelly of the White Knight stub pylon forward fuselage attach point. The aircraft geometry forward of the test section provided a very clean aerodynamic environment with little disturbance of incoming air flow. The White Knight is powered by two Pratt and Whitney J-85 engines with afterburner. Thrust capabilities of these engines at high altitude allowed testing at velocities up to Mach 0.55 at 40,000 ft. This was essentially the required Mach at the lowest possible altitude. Prior to testing, concern was expressed that the acoustic levels of these engines (even without afterburner) could interfere with laminar flow; however, laminar flow performance did not appear to be affected by acoustic disturbances.

Before attaching the model to the White Knight's pylon all cables were routed into the fuselage through an access port in the stub pylon. After the installation of the model, power and instrumentation components were secured inside the airplane's aft fuselage section. The data acquisition and control laptop and the video DVR were secured to the third seat in the forward cockpit for access by the co-pilot. All systems were then taken through ground testing and evaluation prior to flight testing.

Test flights were performed over the Isabella MOA airspace. Flight testing was conducted at two primary test points: Mach 0.40 at 25,000 ft and Mach 0.55 at 40,000 ft – with the Mach 0.55 case being the primary case of interest. The Reynolds number at the 25,000 ft test point was 3.3 million; the Reynolds number at the 40,000 ft test point was 2.8 million.

Flight test procedures were strictly followed for safety and quality of data. Prior to flight, all model sensor and data acquisition and servo controls were given a thorough systems check and the model was wiped down – paying careful attention to clean any bugs or debris off the leading edge. After the model cleared this check, the aircraft

was given a green light to fly. A pre-flight test meeting was held to discuss the model testing, aircraft altitude, Mach, and flight patterns to occur that flight. The aircraft was then rolled out of the hangar and prepped for flight. A two-man crew served to fly the aircraft and operate the MACW system. With the aircraft ready, both engines were started and the model power was switched over to the main generator bus. A final servo check was performed and a “begin flight zero-reference” data point is collected (gathering all sensor data) prior to take-off. At the end of each flight, an “end flight zero-reference” was also taken to look for any sensor drift over the course of testing. Also at the end of each flight, the model leading edge was thoroughly inspected for bug strikes and a post flight model systems check was performed.

The flight test plan consisted of envelope expansion, natural laminar flow testing and high rate flap demonstration. During envelope expansion, the stability and handling qualities of the White Knight were evaluated at various Mach and altitude test points. At each altitude, the pilot performed a series of maneuvers including stick raps at increasing speed, steady heading sideslips with the wing re-configured to its maximum lift setting and its minimum lift setting, and finally a 2.5 G pull-up maneuver.

After the model handling qualities were cleared at all altitudes and speeds, Natural Laminar Flow testing was conducted. The natural laminar flow test matrix consisted of 36 test points designed to measure the model lift, drag and pitching moment. Due to the model’s finite aspect ratio, the angle of attack of the model was significantly elevated over the infinite span CFD predictions. This leads to rather high model angle of attack positions to push the lift range into the desired CL = 0.4 to 1.1 range. Table 1 shows the NLF test matrix for the 40,000 ft test altitude. The data acquisition and control system allowed a test point scheduler to automatically load the next test point in sequence which allowed testing to proceed more quickly.

Table 1. AOA and flap deflections for the NLF test matrix.

<i>NLF Test Matrix for Test Point A (Mach 0.55 @ 40k ft)</i>					
<i>Lift and Moment Forces</i>					
AOA (deg) range	Flap (deg)	Estimated CL range	Estimated Lift (lb) range	Estimated CM range	Estimated Pitching Moment (ft-lb) range
2, 4, 6, 8, 10, 12	-5.0	0.11 to 0.92	130 to 714	0.02 to -0.003	37 to -6
2, 4, 6, 8, 10, 12	0	0.36 to 1.16	284 to 902	-0.06 to -0.08	-119 to -148
2, 4, 6, 8, 10, 12	+2.5	0.47 to 1.21	364 to 945	-0.10 to -0.11	-187 to -215
2, 4, 6, 8, 9, 10	+5.0	0.57 to 1.19	448 to 932	-0.13 to -0.15	-254 to -282
2, 4, 6, 7, 8, 9	+7.5	0.68 to 1.19	530 to 931	-0.17 to -0.18	-333 to -354
2, 4, 5, 6, 7, 8	+10.0	0.76 to 1.18	592 to 917	-0.21 to -0.22	-412 to -426

IV. Flight Test Results

Flight testing occurred during the months of October 2006 and December 2006. The weather in Mojave, CA was very good over the course of testing and there was rarely a day were testing could not be performed due to weather related issues. In some cases an altitude had to be modified to move away from cloud layers in order to keep ice crystals from forming on the leading edge. By working with Scaled pilots, a sideslip tolerance of +/- 1 degree (which was AOA for the model) and a velocity tolerance of +/- 2 knots. In smooth air, these tolerance were held to tighter levels than these criteria. Turbulence, however, made holding tolerances more challenging. The onboard data acquisition systems on the White Knight and the MACW model allowed speed, altitude, and sideslip variability to be monitored. Bug strikes on the leading edge were practically nonexistent – only 3 bug strikes were observed on the leading edge during the entire 27 hours of flight testing.

E. Model Surface Pressures

Figure 8 and Figure 9 show the model surface pressures at the Mach 0.55 case at 40,000 ft. In Figure 8, the angle of attack is held constant and the flap is deflected to increase the lift generation of the wing. As the flap is deflected, the wing produces more and more lift; however, the pressure gradient on the upper surface over the first 60% of the model chord remains favorable thus keeping the boundary layer laminar. At roughly 60% model chord, the airfoil geometry contains a subtle bump in the upper surface to trip the boundary layer – as a turbulent boundary layer is “stickier” than a laminar boundary layer and can maintain attachment to the trailing edge surface over larger

adverse pressure gradients. The steepness of the adverse pressure gradient in this model necessitates a smooth, variable geometry surface to maintain flow attachment – even when flap deflections are small.

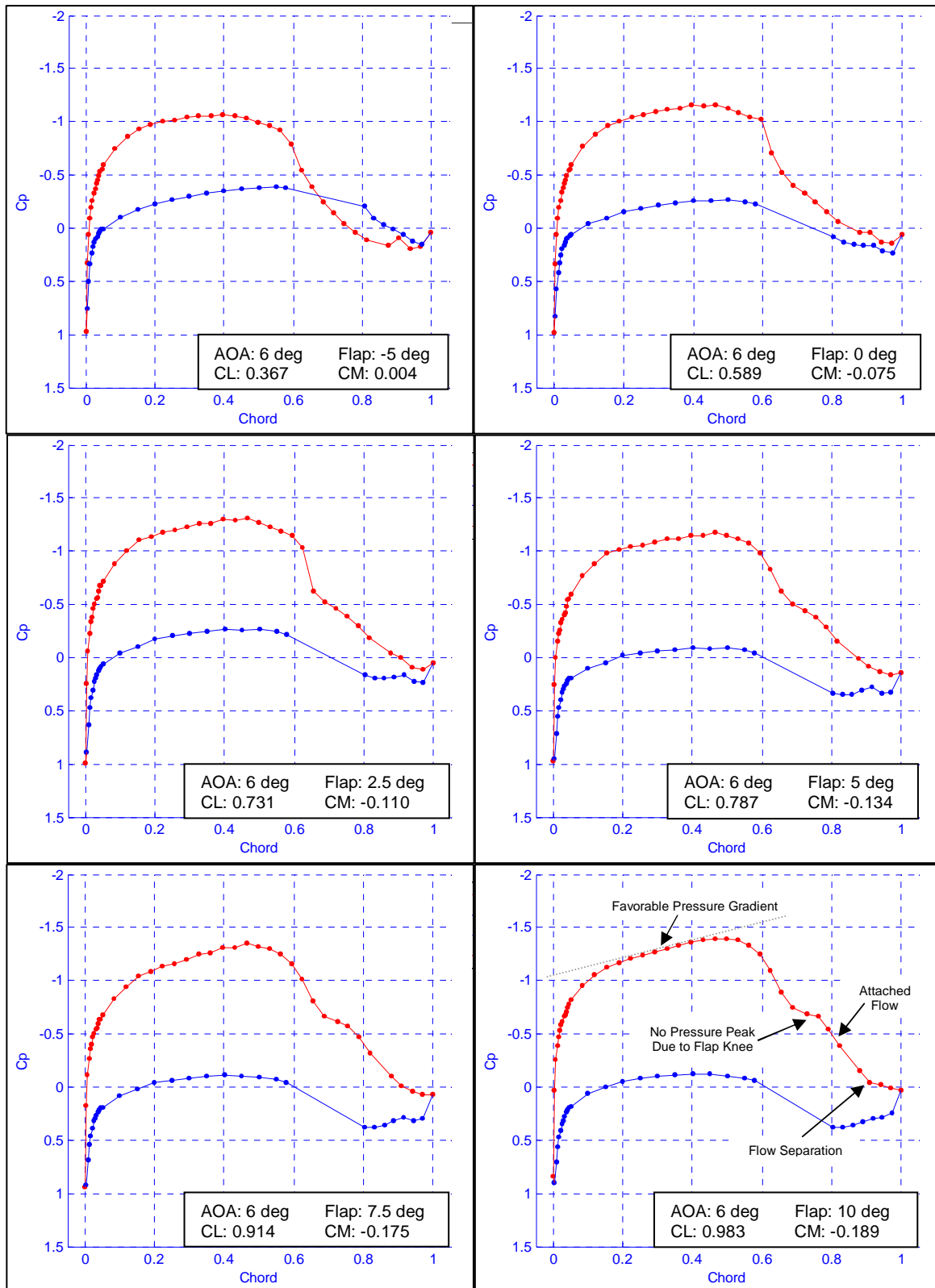


Figure 8. Cp plot for constant AOA and changing flap deflection.

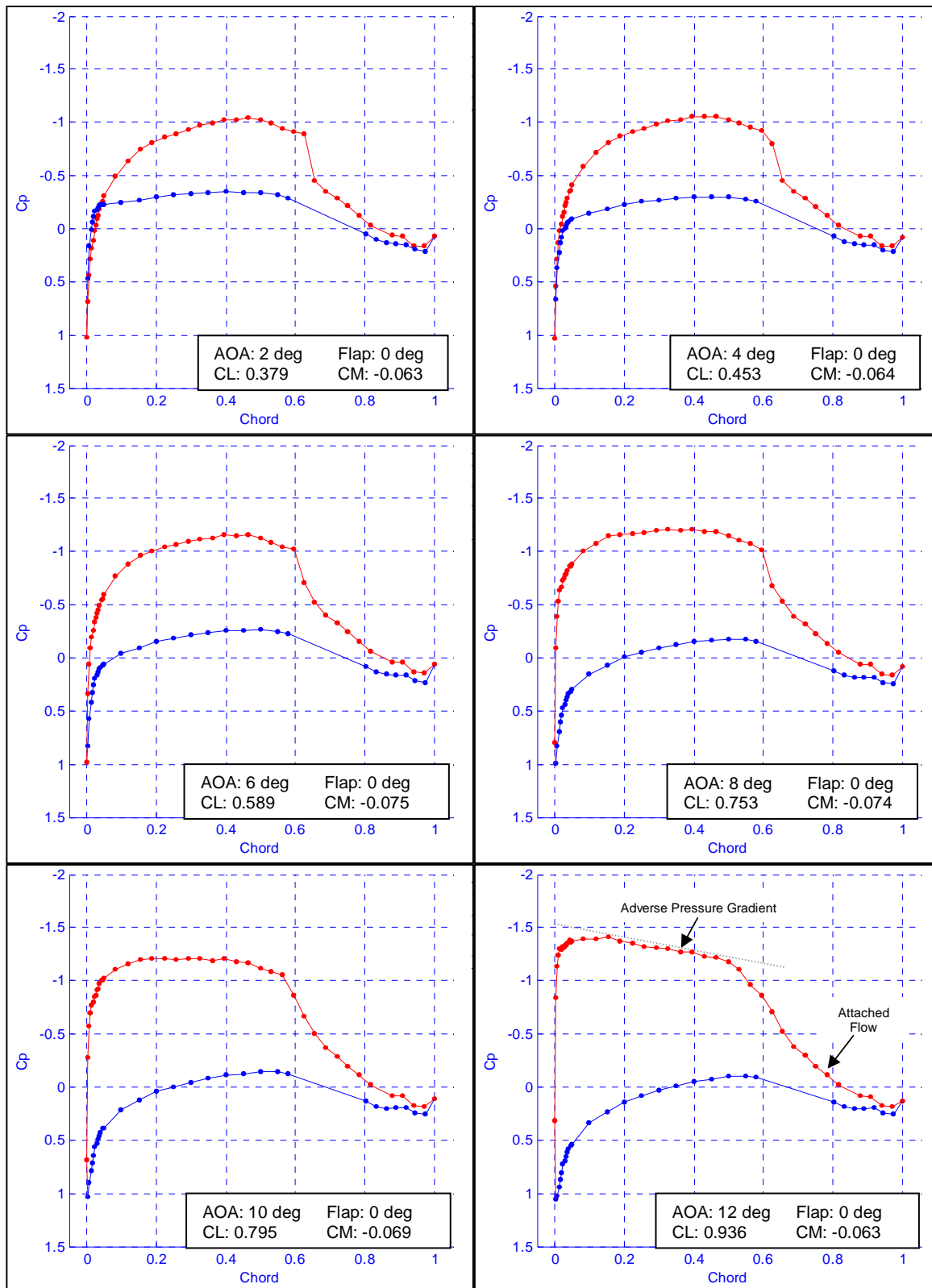


Figure 9. C_p distribution with flap fixed at 0 degrees and AOA varied to change lift levels.

In contrast to the case where the AOA is held constant and the flap is deflected, Figure 9 displays the C_p curves as the flap is held constant and the AOA is increased to vary the lift production. The first 3 angles of attack from 2

degrees to 6 degrees maintain a favorable pressure gradient on the upper surface. The CP curve for the angle of attack of 8 degrees and 10 degrees maintain a marginal pressure gradient on the upper surface. The CP curve for the angle of attack of 12 degrees, required to achieve a lift coefficient of 0.936 has an adverse pressure gradient after the leading edge suction peak – promoting turbulent transition of the boundary layer.

F. Model Hot-Film Data

Hot film data was primarily tracked for the model upper surface. Hot films heat a very thin nickel resistive element deposited on a Kapton film to 100 to 150 degrees Celsius. A constant probe temperature is maintained by using carefully derived probe resistance measurements and a measure of the probe’s change in resistance per ΔT . Feedback control is performed by the Constant Temperature Anemometer (CTA) which can track up to 8 separate probes simultaneously (each probe has a separate resistance and percent resistivity measurement). A laminar boundary layer (versus a turbulent boundary layer) has a lower rate of convection and a much lower velocity variance. These physical differences show up as changes in the voltage signal output from the CTA (voltage signal is proportional to the probe current).

Hot film data was gathered at 1000 Hz for 8 seconds for each of the 8 films on the upper surface. By comparing a film’s voltage amplitude for a “zero White Knight velocity” condition and a “turbulent reference condition” (generated by placing a 0.005” trip strip on the model 5% chord and flying the model at several representative test points), we can qualitatively determine whether the boundary layer is laminar or turbulent. Note that a boundary layer does not instantly transition from laminar to turbulent and there are typically intermittency regions where the boundary layer is not consistently laminar or turbulent. Those regions are identified by bursting between a laminar signal and a turbulent signal.

Hot film data signals are plotted in Figure 10 for the case of 0 degree flap and 6 degree AOA ($CL = 0.589$), Figure 11 for 0 degree flap deflection and 12 degree AOA ($CL = 0.936$) and Figure 12 for 10 degree flap deflection and 6 degree AOA ($CL = 0.983$). Note that the average value of each signal is shifted to avoid overlapping voltage signals. The lower Reynolds number associated with flight testing at 40,000 ft provided a relatively resilient boundary layer and laminar runs could be achieved even with a fairly unfavorable pressure gradient.

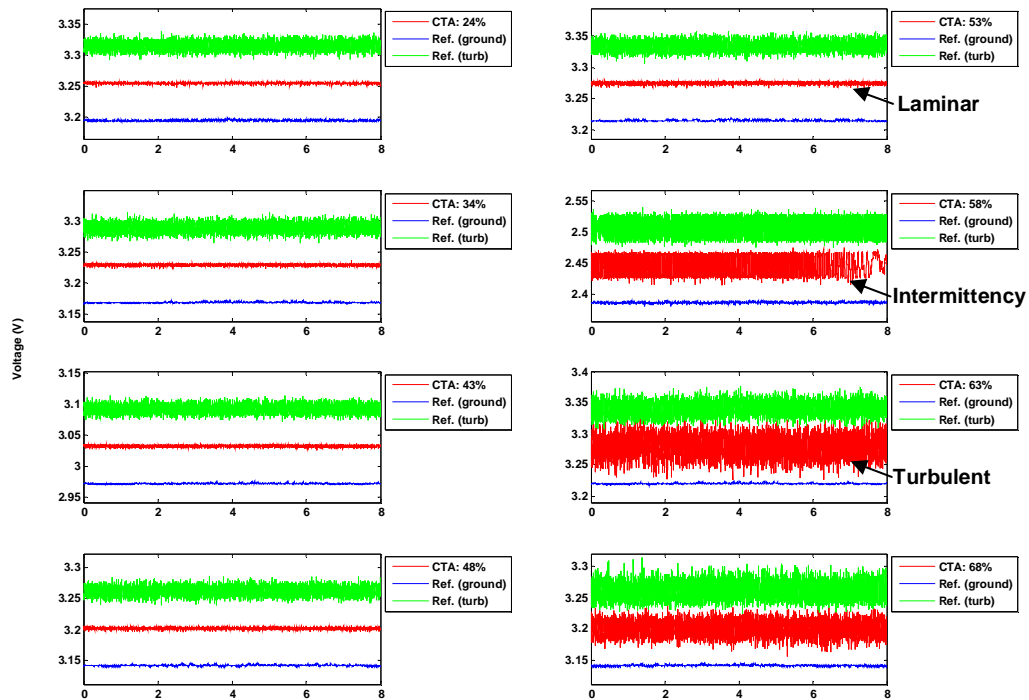


Figure 10. Hot film signals for 0 degree flap deflection and 6 degree AOA.

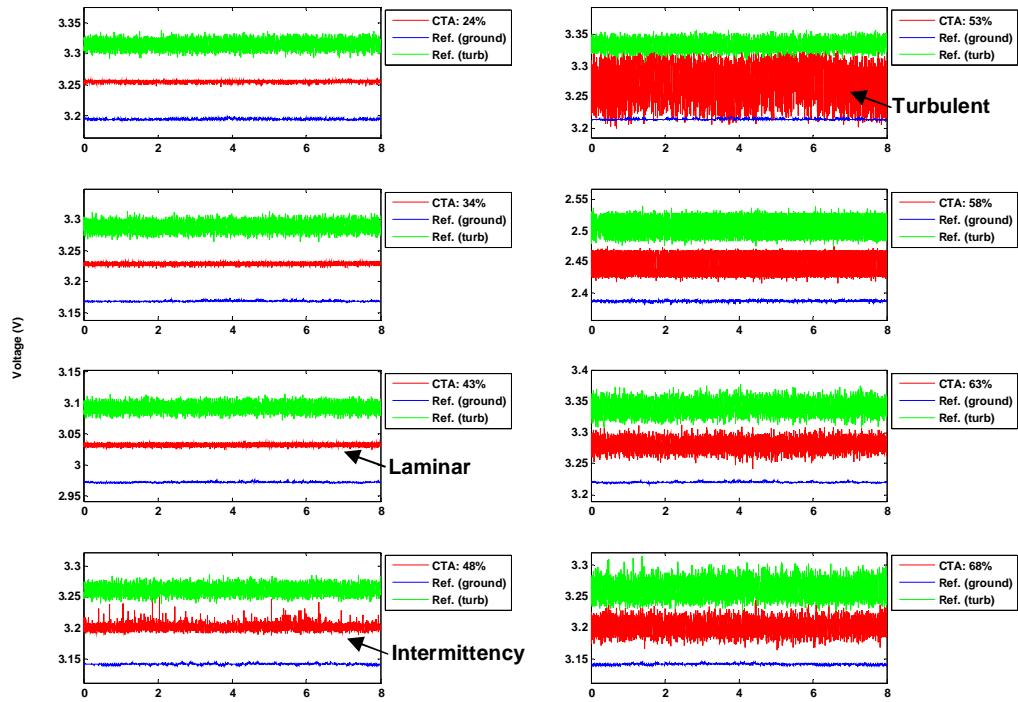


Figure 11. Hot film signals for 0 degree flap deflection and 12 degree AOA.

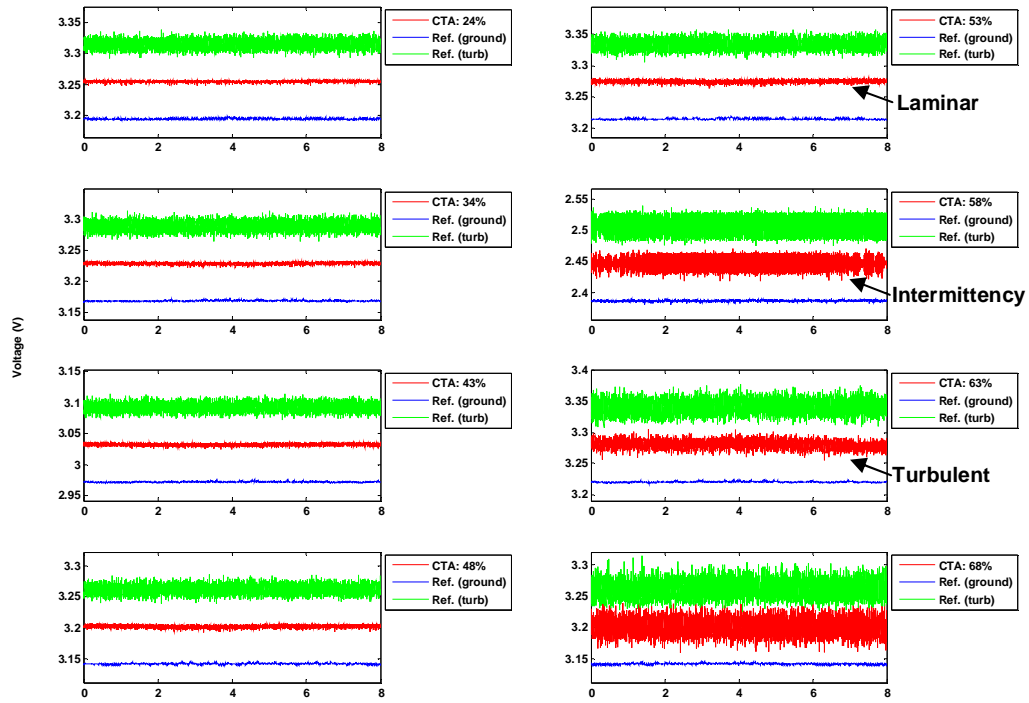


Figure 12. Hot film signals for +10 degree flap deflection and 6 degree AOA.

Figure 10 shows a typical case with the boundary layer remaining laminar through 53% chord. At 58% chord, the boundary layer is primarily turbulent but with a sharp drop in signal amplitude near the end of the 8 seconds which signals an intermittency region. At 63% of the chord and beyond, the boundary layer is consistently turbulent. For the case of 0 degree flap and 12 degree AOA, Figure 11 shows laminar flow through 43% chord, the intermittency region beginning at 48% chord, and the turbulent region occurring at 53% chord.

In contrast, the hot film plot in Figure 12 with the flap at 10 degrees and the AOA at 6 degrees shows the intermittency region beginning at 58% chord and becoming fully turbulent at 63% chord. Thus even at these higher lift levels, laminar flow is maintained for roughly 10% longer using the flap to generate lift rather than using the model angle of attack. Operation of the model at higher Reynolds numbers would likely make this change in laminar flow discrepancy significantly larger.

G. Model Aerodynamic Polars

Polars are plotted for the model lift versus angle of attack (Figure 13) and pitching moment versus angle of attack (Figure 14), and finally for the model lift to drag behavior (Figure 15). This data is compared to MSES [REF] two-dimensional, infinite span results for wing at the same Mach 0.55, RN = 2.8 million. The largest discrepancy is that the lift-to-AOA slope is significantly different. Also the change in the lift coefficient per unit flap deflection is also much less than predicted by 2D CFD. The reason for these discrepancies is due to finite aspect ratio of the model. With no endplates, the model maintains an aspect ratio of 1.67; however, the elliptical endplates increase this aspect ratio. Using Equation 1 [REF Theory of Wing Sections], we compute our model's finite aspect ratio to be 4.45. Thus the elliptical endplates improve the wing's aspect ratio from 1.67 to 4.45. Larger endplates would have increased the aspect ratio further; however, the drag of the model would have increased above the point where the Mach 0.55 speed was achievable.

$$\alpha' = \alpha + \frac{C_L}{\pi A} \quad (1).$$

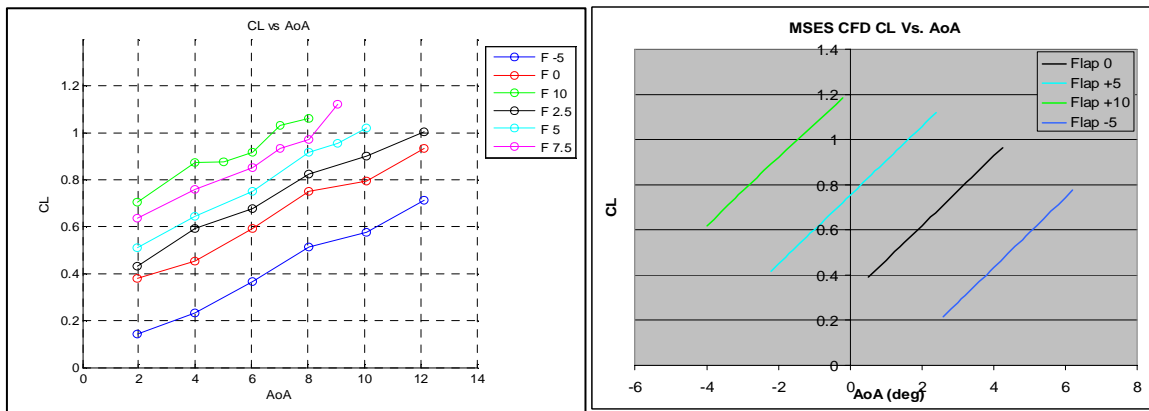


Figure 13. CL Vs. AOA experimental data for the varying flap deflections compared to MSES 2D CFD predictions.

The finite aspect ratio also decreases the effectiveness of the flap. For the MSES case, a flap deflection of 5 degrees produces an offset in CL of 0.088 per degree flap deflection. The experimental data revealed an offset in CL that measured 0.036 per degree flap deflection. Thus, the finite aspect ratio behavior also affects the flap effectiveness.

Moment predictions as compared to MSES 2D CFD are also displayed below. The primary shift in moment production occurs at much lower and more compressed ranges of angle of attack. The magnitudes of the moment production are largely unaffected by the finite aspect ratio and wing camber and pitching moment agree relatively well with MSES predictions. Deflecting the flap produces a significant pitching moment. In practice, this pitching moment would be counteracted by correctly trimming the aircraft.

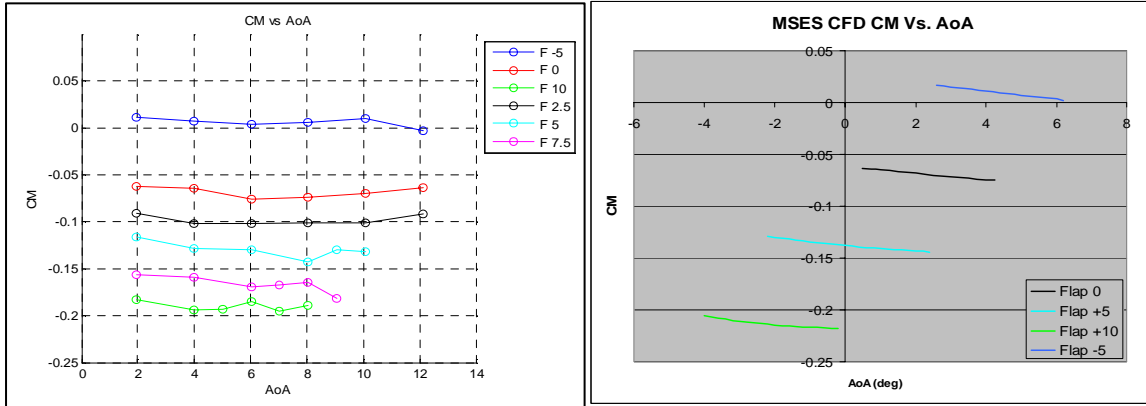


Figure 14. CM Vs. AoA experimental data for the varying flap deflections compared to MSES 2D CFD predictions.

Drag measurements during experimental flight testing are accomplished by sweeping three pitot probes behind the model to survey the momentum deficit. The rotating arm wake rake was favored over a rake fixed to the trailing edge flap due to the ability of the wake to move with respect to model flap deflection and angle of attack. Drag coefficients are calculated using A.D. Young’s form of the drag equation which accounts for the non-zero static pressure field behind the model as well as compressibility (which is slight at Mach 0.55). The drag equation [REF – Schlichting book on boundary layers] is shown below:

$$c_D = 2 \int_{-\infty}^{+\infty} \sqrt{\frac{g_2 - p_2}{q_\infty}} \left(1 - \sqrt{\frac{g_2 - p_\infty}{q_\infty}} \right) \left\{ 1 + \frac{M_\infty^2}{8} \left[3 \frac{p_2 - p_\infty}{q_\infty} + 3 - 2\gamma - 2 \frac{g_2 - p_\infty}{q_\infty} - (2\gamma - 1) \sqrt{\frac{g_2 - p_\infty}{q_\infty}} \right] \right\} d \left(\frac{y}{l} \right) \quad (2).$$

Drag polars for the experimental and CFD results are also displayed in Figure 15 for the lift coefficient ranges explored during testing.

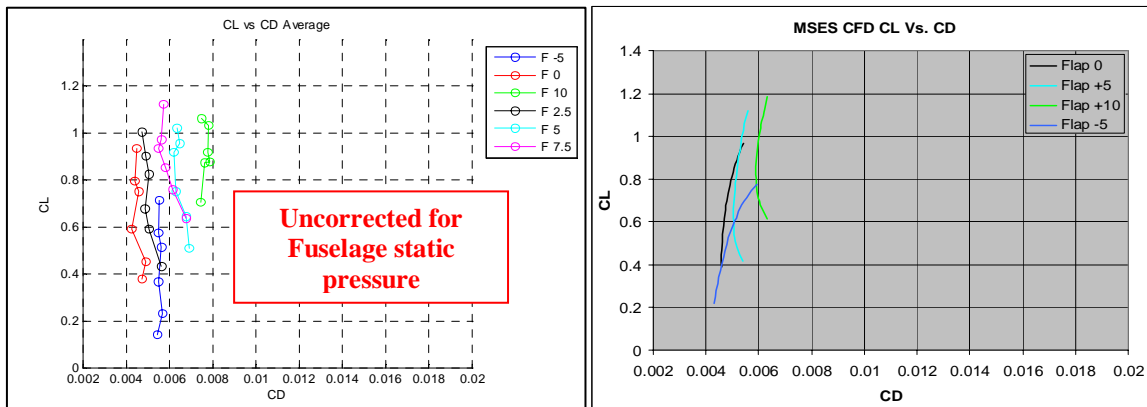


Figure 15. CL Vs. CD for varying flap deflections compared to MSES 2D CFD predictions.

Drag levels are shown to compare reasonably well with predicted MSES calculations. According to measurements, the MACW wing appeared to have slightly higher drag levels than predicted by MSES. The thinking behind this is that the wing did not quite achieve the percentage chord laminar flow as predicted by MSES. Also, the fact that the intermittency region occupies 5% to 10% of the model chord is also not modeled in MSES. Nevertheless, the experimental results compare very favorably opening the door to future designs at elevated Reynolds and Mach numbers.

H. High Rate Flap Testing

Because the MACW technology is primarily limited by the speed of the internal actuator (brushless DC servomotors in this embodiment), high flap deflection rates are achievable. The conclusion of the testing involved a

high rate demonstration at flap rates up to 30 degrees per second. These rates are compatible with performing Gust Load Alleviation (GLA) for SensorCraft vehicles to alleviate high moment loading (and high stresses) in the wing box. This GLA concept can allow for considerable weight to be pulled from the aircraft wing, allowing further gains in range and endurance. The following figures depict the wing at 25,000 ft Mach 0.4 moving at a maximum velocity of 30 degrees per second. The success of the high rate capability of the MACW model shows the great potential of this technology to impact SensorCraft and many other aircraft that can benefit from the variable geometry capability.

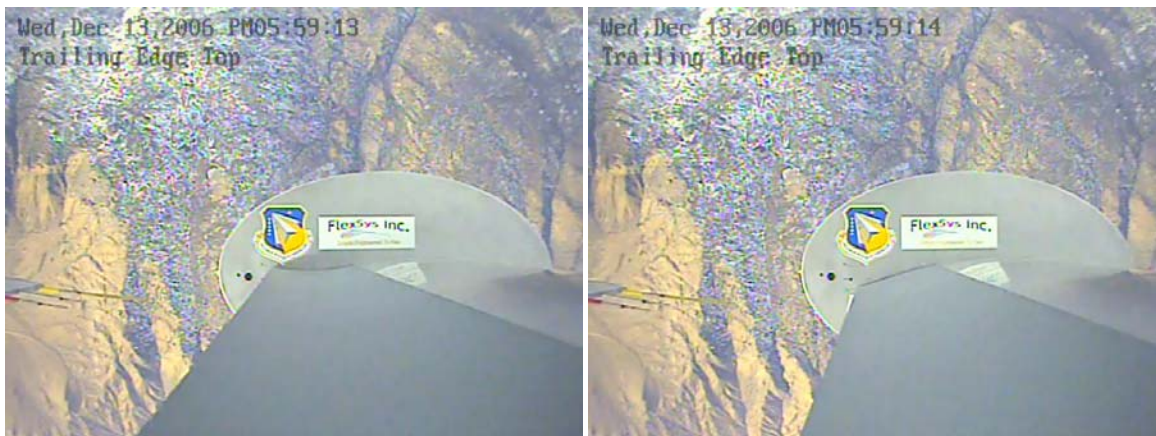


Figure 16. View from inboard endplate camera showing trailing edge upper surface moving from -10 degrees to +10 degrees at a 30 degree per second rate.

V. Conclusions and Recommendations

The aerodynamic data (lift, drag and moment) measured during the flight test program agreed quite well with the predicted levels determined computationally by AeroCraft using the MSES5-1 code when corrections for test model aspect ratio were taken into account. At the higher Mach flight test point, $M = 0.55$, $h = 40k$ ft., The test airfoil drag level tracked the predicted level across the entire airfoil operating lift range with some minor deviations in the airfoil high lift area. Further, the Dantec hot film sensor measurements on the wing upper surface confirmed extensive runs of laminar flow even at high operating lift conditions.

These lift levels are both achievable while maintaining 60% chord (or greater) laminar boundary layer runs. The mission adaptive compliant flap can effectively control the upper surface pressure distribution while maintaining a sufficiently large transition radius into the pressure recovery region. This geometry minimizes flow separation and drag.

I. Endurance Aircraft Applications

The MACW flight validation experiment successfully demonstrated that an adaptive compliant trailing edge flap can be successfully designed, manufactured, and operated in an atmospheric environment compatible with long endurance military aircraft mission requirements. And while it is difficult to determine the exact impact MACW technology might have on specific endurance aircraft without first knowing the configuration, prior Air Force sponsored studies [REF 5-2] have shown that constant altitude endurance flight may be required while carrying a fuel load of 45% to 55% of aircraft gross weight. The ability to operate at minimum drag over lift ranges is essential for mission success. Examining aerodynamic improvement alone, MACW technology has the potential for increasing the endurance of these air vehicles 15% or more, or alternately reducing fuel burn by a like amount. If gust load alleviation is taken into account – the ability of the flap to twist along the span to further lower wing root bending moment – further weight savings are suitably envisioned.

Mission adaptive compliant wing technology has been brought to a technology readiness level that will support its application on the next generation high altitude long endurance aircraft. As demonstrated during the flight test program the overall mission performance benefit of a carefully integrated variable camber trailing edge can be substantial. During flight testing, the MACW model was demonstrated at full scale dynamic pressure, Mach, and reduced scale Reynolds numbers. The flap was successfully operated in a high altitude, low temperature environment and did not encounter any operational restrictions or limitations. A final validation of MACW design/fabrication technology to consider might be actually replacing a trailing edge surface on a flying endurance

aircraft with a compliant flap/control. A program of this type would demonstrate fully aircraft structural integration and resolve any remaining weight and actuation issues.

J. Transonic Cruise Aircraft Applications

With jet fuel prices high and, if current trends are any indication heading higher in the foreseeable future, now is the time to aggressively pursue fuel savings technology on all fronts. FlexSys and others, for example [REF 5-3, 5-4], have studied the integration of a variable camber trailing edge to commercial transport aircraft for mission L/D optimization. Aerodynamic results from these studies were quite promising as indicated in Figure 17.

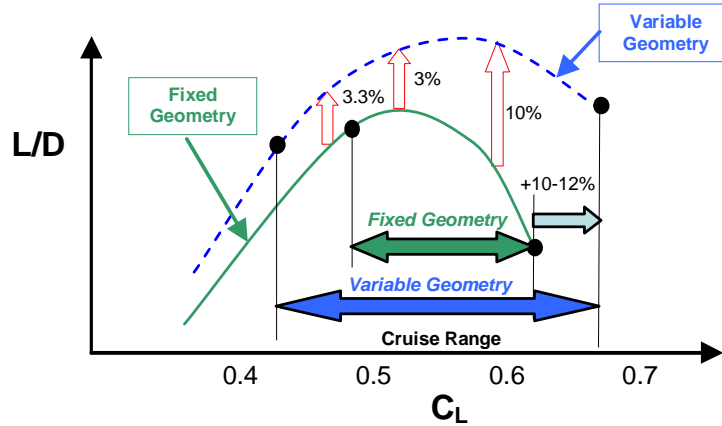


Figure 17. L/D improvement (Airbus A320) with variable geometry trailing edge.

These results, taken from REF [REF 5-4], appeared to offer a substantial mission performance improvement (fuel savings), but the variable geometry implementation required moving, and holding in position, the high lift trailing edge during high “q” cruise conditions. The resulting weight penalty in the flap structure/actuation system reduced the estimated performance improvement by one half in the heart of the cruise performance envelope.

Taking a lead from the Northrop-Grumman study [REF 5-3 Comparison of smart-wing concepts for transonic cruise drag reduction] FlexSys has conceptualized a trailing edge concept that integrates cruise variable camber into the aft element of the high lift flap as shown in Figure 18.

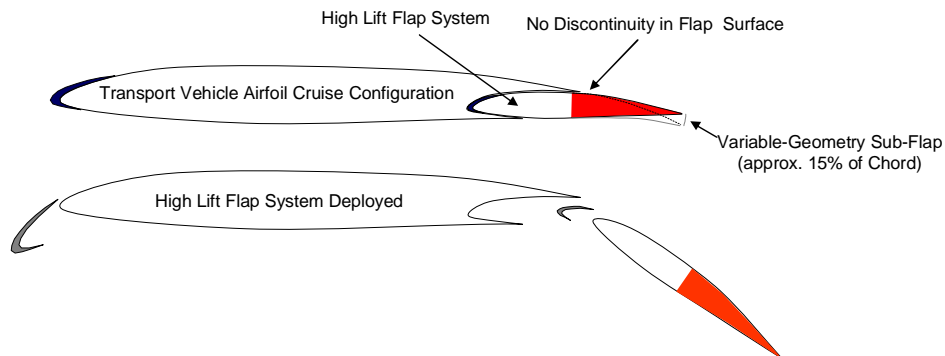


Figure 18. FlexSys high lift flap with cruise variable geometry feature.

The compliant structure, variable geometry addition to the aft flap element can provide camber control needed to produce performance levels similar to those presented in Figure 18 at an acceptable weight penalty. For example, a medium range transonic transport incorporating the flap system shown is projected to save over 100 gallons of jet fuel on a cross country flight (compliant flap cruise L/D improved 3.3). Depending on aircraft utilization fuel saving of 64,000 gal/yr per aircraft is not an unreasonable estimate.

A flight validation program to verify variable geometry cruise control performance enhancement on a transonic transport aircraft configuration would be beneficial to both future military and commercial aircraft development programs.

Acknowledgments

FlexSys Inc. is grateful for the support of Air Force Research Lab VAAA in funding this work. Their continued support has allowed significant and rapid maturation of the MACW technology. FlexSys would also like to thank Hal Youngren of AeroCraft for his tireless work and contribution to the program and to Lockheed Martin for their technical support and input to the model design. Finally FlexSys would like to thank Scaled Composites for their time and talent in helping make the flight test a success.

References

¹Tilman C.P., Flick P.M., Martin C.A., Love M.H., “High Altitude Long Endurance Technologies for SensorCraft”. RTO AVT Symposium on “Novel Vehicle Concepts and Emerging Vehicle Technologies”, held in Brussels, Belgium, 7-10 April 2003, and published in RTO-MP-104.

²Kota, S., Hetrick, J., Osborn, R., Paul, D., Pendleton, E., Flick, P. and Tilman, C., “Design and Application of Compliant Mechanisms for Morphing Aircraft Structures,” Paper 5054-03 SPIE Smart Structures and Materials Conference on Industrial and Commercial Applications of Smart Structures Technologies, San Diego CA, 2-6 March 2003.

³Reed, S.A., “High Altitude Long Endurance Airfoil Performance Validation”, WL-TR-96-3091, Flight Dynamics Directorate, Wright Laboratory, Wright-Patterson AFB, OH, January 1996.

Add more references...